JOURNAL OF CATALYSIS **135**, 618–634 (1992)

Infrared Study of the CO Insertion Reaction on Reduced, Oxidized, and Sulfided Rh/SiO_2 Catalysts

STEVEN S. C. CHUANG[1] AND SHYH ING PIEN

Department of Chemical Engineering, The University of Akron, Akron, Ohio 44325

Received October 2, 1991; revised January 28, 1992

The reaction of adsorbed CO with C_2H_4/H_2 and ethylene hydroformylation over reduced, oxidized, and sulfided Rh/SiO_2 catalysts has been investigated under reaction conditions by *in situ* infrared spectroscopy. Both reactions involve the CO insertion step resulting in the formation of propionaldehyde. The linear CO adsorbed on the Rh^0 site of the reduced Rh/SiO_2 and the linear CO adsorbed on the Rh^+ site of the oxidized Rh/SiO_2 are consumed and propionaldehyde is produced as the adsorbed CO reacts with C_2H_4 and H_2. The results show that both single Rh^0 atoms and Rh^+ ion sites are active for the CO insertion reaction. *In situ* infrared observations of steady-state ethylene hydroformylation show that the oxidized Rh/SiO_2 containing considerable amounts of Rh^+ sites exhibits rate and selectivity for the formation of propionaldehyde higher than those of the reduced Rh/SiO_2; the sulfided Rh/SiO_2 comprising mainly single Rh sites shows rate and selectivity for the formation of propionaldehyde higher than that of the reduced Rh/SiO_2. The low selectivity of the reduced Rh/SiO_2 for ethylene hydroformylation is attributed to the high hydrogenation activity of the Rh crystallite surface on the reduced Rh/SiO_2. © 1992 Academic Press, Inc.

INTRODUCTION

The insertion of carbon monoxide (CO) into a metal–carbon σ bond is one of the most widely studied reactions in organometallic chemistry (*1*). The interest in CO insertion stems from the fact that the reaction provides a pathway for the conversion of olefins or other substrates to high added-value chemicals (*1, 2*). Homogeneous hydroformylation processes have been the largest industrial application of the CO insertion chemistry for more than three decades (*3–5*). Although Rh carbonyls and complexes are the most active hydroformylation catalysts, mechanistic information about CO insertion has commonly been obtained using metals such as Mn, Ir, or Pt, which form unreactive and stable acyl complexes (*2*). The use of these organometallic complexes allows close observation of how the migratory CO insertion occurs. Infrared study of the ^{13}CO insertion on alkyl(pentacarbonyl)-manganese has provided direct evidence of the migratory insertion of CO into a carbon–metal bond on Mn^+ (*6*). The rate of CO insertion on methyl(pentacarbonyl)-manganese can be further accelerated by a Lewis acid (*7*).

It has been suggested that the migratory CO insertion plays a key role in the Fischer–Tropsch (F–T) synthesis (*8, 9*). Pichler *et al.*(*8*) first used CO insertion as a model for rationalization of chain growth in the F–T catalysis on surfaces. However, most F–T studies over the past decade have shown that CO insertion is not the major pathway for the chain propagation of adsorbed alkyl (*10–15*). The CO insertion step was found to be the chain termination step leading to the formation of aldehydes and alcohols (*14–21*).

While it has been well established that CO insertion occurs via the migration of an alkyl group to a Rh^+-coordinated CO in homogeneous catalysis (*1–6*), much controversy exists concerning active sites for CO insertion in the CO hydrogenation reaction (F–T syn-

---

[1] To whom correspondence should be addressed.

0021-9517/92 $5.00

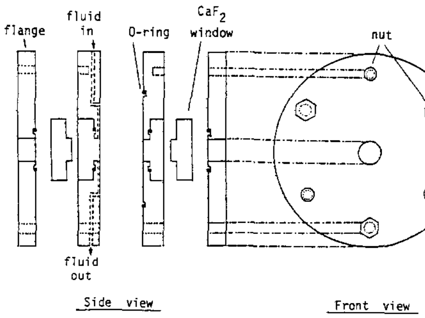

FIG. 1. High-pressure IR cell for *in situ* IR studies.

thesis). Watson and Somorjai (*16, 17*) proposed that CO insertion to form C_{2+} oxygenates occurs on the Rh^+ sites while CO dissociation takes place on the reduced Rh^0 sites. The postulate has been further supported by a number of studies (*18–20, 22–24*). On the contrary, Katzer *et al.* reported from an XPS study that there was no evidence for the existence of Rh^+ on Rh/TiO$_2$, which was active for the synthesis of C_2 oxygenates (*25*). A number of studies have shown no correlation of C_{2+} oxygenate activity to the amount of Rh^+ or Rh^{n+} ions present on the Rh catalysts (*26, 27*).

The present study was aimed at identification of the type of adsorbed CO species that participates in the CO insertion step in ethylene hydroformylation. The Rh catalyst system chosen for this study comprises three different forms of Rh: reduced Rh, oxidized Rh, and sulfided Rh. The types of CO adsorbed on these Rh surfaces are closely related to the surface states of Rh (*28–35*). Infrared data for CO adsorption on these Rh catalysts under various reaction conditions were obtained to determine the type of adsorbed CO for CO insertion and to shed light on the nature of active sites for the reaction.

EXPERIMENTAL

CO adsorption, the reaction of preadsorbed CO with C_2H_4 and H_2, and ethylene hydroformylation on Rh catalysts were carried out in an infrared (IR) cell. The IR cell, shown in Fig. 1, consists of four stainless-steel flanges, a gas inlet and outlet, and two step CaF$_2$ windows. The IR cell can be operated at temperatures up to 533 K and at a pressure of 60 atm. The step windows minimize the reactor volume and reduce the optical path length for the gaseous species in the reactor. Infrared spectra were measured by a Nicolet 5XSC FTIR spectrometer with a DTGS detector at a resolution of 4 cm^{-1}.

A 3 wt% Rh sample was prepared by impregnation of SiO$_2$ (Strem Chemicals, No. 14-7420; SA, 350 m^2/g) with an aqueous solution of $Rh(NO_3)_3 \cdot 2H_2O$ (Johnson–Matthey Chemicals). After impregnation, the sample was dried overnight in air at 301 K and then reduced in flowing hydrogen at 673 K for 16 h. The crystallite size of Rh was determined to be 96 Å by hydrogen chemisorption. The reduced Rh/SiO$_2$ sample was pressed into a self-supporting disk (20 mg, 10 mm in diameter, and 1 mm in thickness) and then placed in the IR cell.

The catalyst disk in the IR cell was subjected to further treatments prior to the adsorption and reaction studies. The treatments included reduction, oxidation, and sulfidation. The catalyst disk reduced in H_2 flow at 513 K for 1 h is designated as the reduced Rh/SiO$_2$ catalyst; the catalyst disk oxidized in flowing air at 513 K for 1 h is denoted as the oxidized Rh/SiO$_2$ catalyst; and the catalyst disk sulfided in H_2S flow (1000 ppm H_2S in H_2) at 513 K for 1 h is designated as the sulfided Rh/SiO$_2$ catalyst. Sulfur content of the sulfided Rh was measured by X-ray fluorescence spectroscopy. The oxidation state of the Rh surface on the reduced and oxidized catalysts was determined by X-ray photoelectron spectroscopy (XPS) using a Leybold LHS-10 surface analysis system.

CO adsorption was conducted by exposing the catalysts to 1–10 atm of CO at 301 K. Gaseous CO was removed by flowing nitrogen. The infrared spectra of adsorbed CO were recorded at 1 atm of CO or N_2. The reactivity of the adsorbed CO was investigated by introducing C_2H_4/H_2 (molar ratio of $C_2H_4 : H_2 = 1 : 1$) to the adsorbed CO

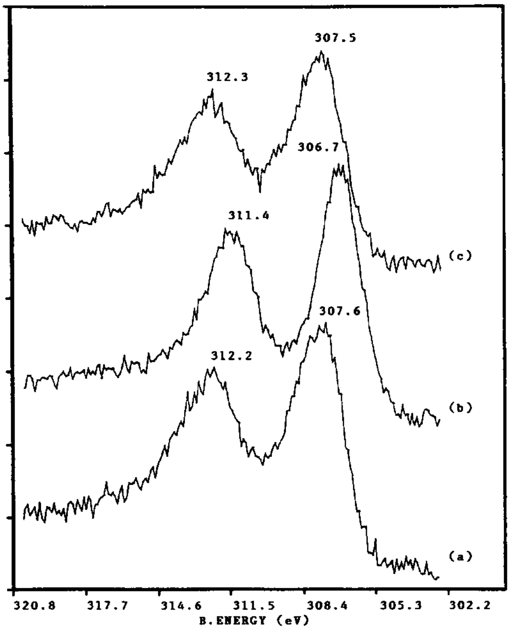

FIG. 2. Rh $3d_{3/2}$, $3d_{5/2}$ XPS spectra of Rh/SiO_2: (a) after exposure to air at room temperature, (b) after reduction in H_2 at 513 K for 3 h, (c) after oxidation in air at 513 K for 3 h.

in the IR cell that served as a batch reactor. The reaction of the preadsorbed CO with C_2H_4 and H_2 was carried out at 301 K and at a pressure of slightly above 1 atm. The infrared spectra of adsorbed CO and intermediates during the reaction were measured as a function of reaction time.

Steady-state ethylene hydroformylation over the reduced, oxidized, and sulfided Rh/SiO_2 catalysts was carried out in the IR cell at 373–513 K and 1–10 atm. Infrared spectra were recorded as a function of time on stream. The effluent of the IR cell was sampled after 40 min at each reaction condition and was analyzed by an on-line HP-5890A gas chromatograph with a 6-ft Porapak PS column in series with a 6-ft Porapak QS column.

RESULTS

X-Ray Photoelectron Spectroscopy

Figure 2 shows the XPS spectra of the Rh/SiO_2 following different treatments. The Rh $3d_{3/2}$ and $3d_{5/2}$ binding energies for the Rh/SiO_2 after exposure to air were observed at 312.2 and 307.6 eV, respectively. Following the reduction at 513 K, the Rh surface was reduced as indicated by the downshift of 0.8–0.9 eV. Subsequent oxidation in air at 513 K shifted the Rh $3d_{3/2}$ and $3d_{5/2}$ binding energies back to 312.3 and 307.5 eV. The difference of 0.8–0.9 eV in binding energy between the reduced and oxidized Rh/SiO_2 clearly indicates that the Rh surface on the reduced Rh/SiO_2 contains primarily Rh^0 atoms; and the Rh surface on the oxidized Rh/SiO_2 comprises mainly Rh^+ ions.

CO Adsorption

Figure 3 shows the infrared spectra of CO adsorption on the reduced Rh/SiO_2 at 301 K. Two intense bands at 2073 and 1898 cm^{-1} are assigned to the linear (terminal) and bridged CO adsorbed on the reduced Rh crystallite surface, respectively. The small band at 2104 cm^{-1} and the shoulder at 2037 cm^{-1} are attributed to the symmetrical and asymmetrical C–O stretching of $Rh^+(CO)_2$, the rhodium gem dicarbonyl. Assignments of these adsorbed CO species agree well with those reported for CO adsorption on supported Rh (*28–35*).

The intensity of the gem-dicarbonyl bands slowly increased with exposure time, but the intensity of the bridged CO band remained essentially constant. A further increase in the intensity of the gem-dicarbonyl bands was observed after exposing the catalyst to 3 atm of CO. The slow development of gem dicarbonyl has been attributed to the disruption of Rh crystallites and the formation of isolated Rh^+ sites (*35, 36*). Removal of gaseous CO by flowing nitrogen caused decreases in the intensity and wavenumber of linear CO and bridged CO bands. The decrease in the CO wavenumber has been attributed to the decrease in dipole–dipole interactions between adsorbed CO species (*32, 37, 38*).

Figure 4 shows the infrared spectra of CO adsorption on the oxidized Rh/SiO_2 at 301 K. The band at 2096 cm^{-1} developed and

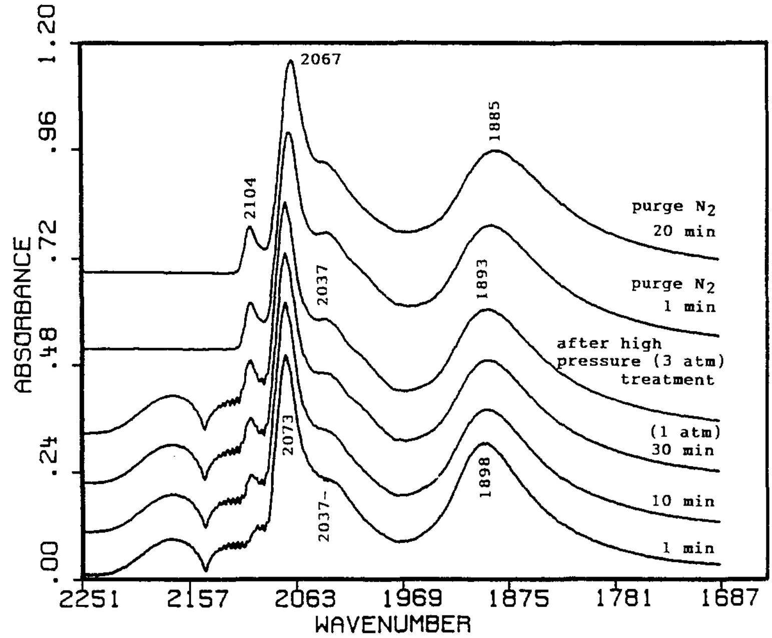

FIG. 3. CO adsorption on the reduced Rh/SiO_2 catalyst at 301 K.

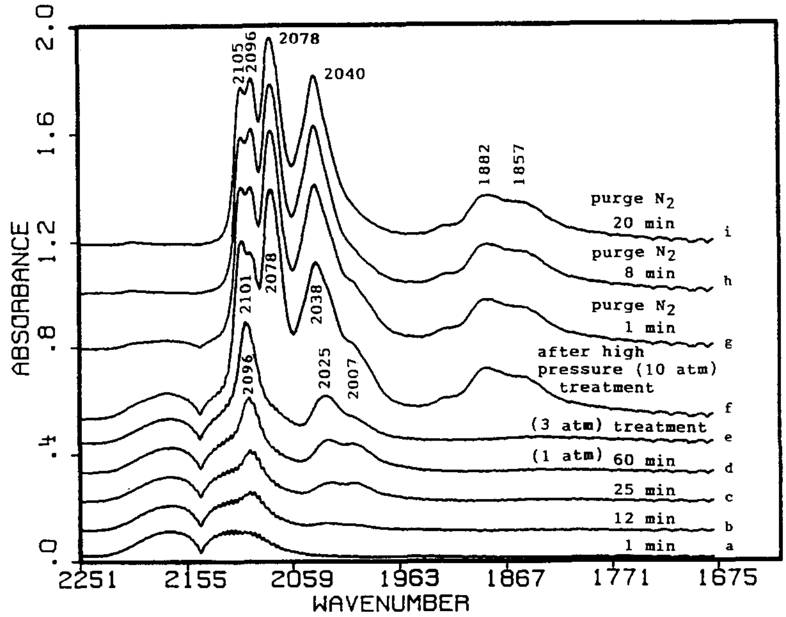

FIG. 4. CO adsorption on the oxidized Rh/SiO_2 catalyst at 301 K.

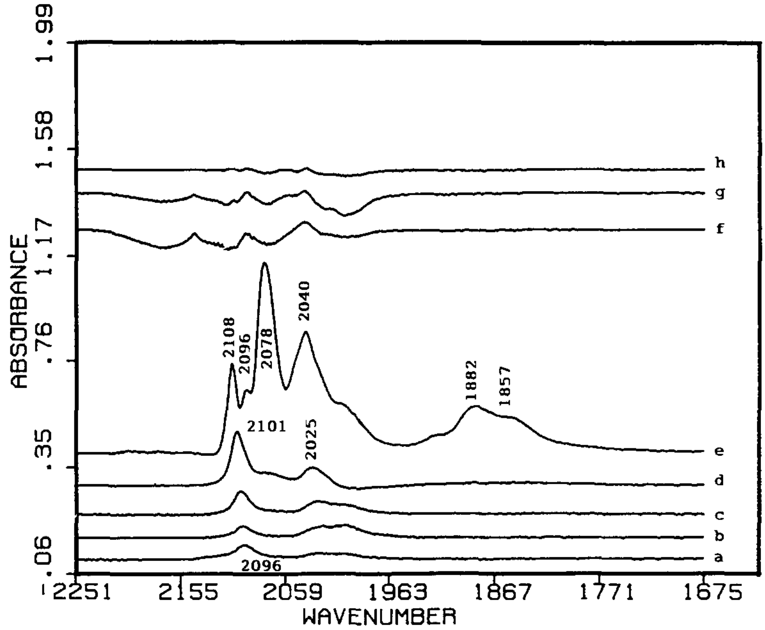

FIG. 5. Sequential difference spectrum of CO adsorption obtained from subtraction of spectra in Fig. 4; spectrum 5a = 4b − 4a, spectrum 5b = 4c − 4b, spectrum 5c = 4d − 4c, etc.

shifted to 2101 cm^{-1} as exposure time increased. A low intensity band at 2025 cm^{-1} also increased in intensity with exposure time. Exposing the catalyst to 10 atm of CO produced a complex infrared spectrum. The development of various IR bands for adsorbed CO species can be clearly discerned in the difference spectra, shown in Fig. 5, which highlights the difference between successive spectra in Fig. 4. The upward shift of the 2096 cm^{-1} band as the intensity increased indicates that the band is not completely due to the symmetric vibration of $Rh^{+}(CO)_2$ because the wavenumbers of symmetric and symmetric bands of $Rh^{+}(CO)_2$ do not change with their intensities (*28–30, 32–35*). The 2096 cm^{-1} band is assigned to the linear CO adsorbed on the Rh^{+} ions. Linear CO adsorbed on Rh^{+} is known to give an IR band in the 2100–2090 cm^{-1} region (*32, 33, 39, 40*). Part of the 2096 cm^{-1} band may be due to the symmetric vibration of $Rh^{+}(CO)_2$, which also gave rise to the asymmetric vibration at 2025 cm^{-1}. The complex spectrum resulting from exposure to 10 atm of CO consists of bands at 2108, 2096, 2078, 2040, 2007, 1882, and 1857 cm^{-1}. The species is quite stable in nitrogen flow. The spectrum does not match with the spectra of various types of Rh carbonyls such as $Rh_4(CO)_{12}$ and $Rh_6(CO)_{16}$ (*5, 41*), nor does the spectrum correspond to those for CO adsorbed on Rh^{2+} and Rh^{3+} sites (*32*). The structure of the resulting complex remains unclear.

Figure 6 shows the infrared spectra of CO adsorption on the sulfided Rh/SiO_2 catalyst at 301 K. CO adsorption produced a band at 2090 cm^{-1}, which may be assigned to a linearly adsorbed CO. Exposure of the sulfided catalyst to CO for 60 min resulted in an increase in the intensity of the linear CO band and an upward shift of its wavenumber of 2095 cm^{-1}. Two bands at 2029 and 2005 cm^{-1} are due to the weakly adsorbed CO on the catalyst surface as indicated by the decreasing intensity of these bands in flowing nitrogen.

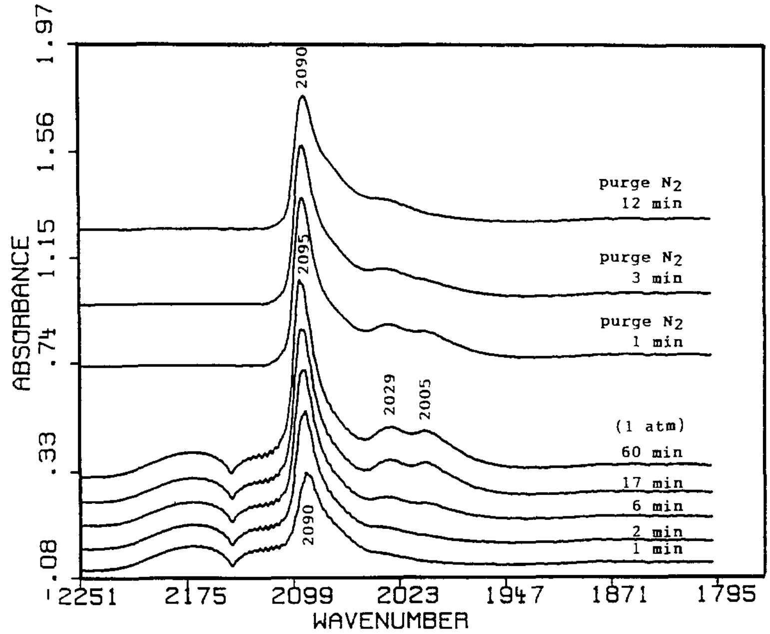

FIG. 6. CO adsorption on the sulfided Rh/SiO$_2$ catalyst at 301 K.

Reaction of Adsorbed CO with C_2H_4 and H_2

Figure 7 shows the infrared spectra taken during the reaction of C_2H_4 and H_2 with the preadsorbed CO on the reduced Rh/SiO$_2$ catalyst at 301 K. The infrared spectrum prior to admission of C_2H_4/H_2 exhibited a linear CO band at 2070 cm^{-1}, a bridged CO band at 1891 cm^{-1}, and gem-dicarbonyl bands at 2104 and 2040 cm^{-1}. Exposure of adsorbed CO to C_2H_4/H_2 decreased the intensity and wavenumber of the linear CO band at 2070 cm^{-1}. At the same time, the propionaldehyde band at 1724 cm^{-1} emerged. A slight decrease in the intensity of gem-dicarbonyl bands was also observed. The consumption of linear CO and the formation of propionaldehyde indicates that the linear CO adsorbed on the Rh^0 crystallite is the major type of adsorbed CO that participates in CO insertion leading to the formation of propionaldehyde at 301 K and 1 atm. The spectra for hydrocarbons in the 2650–3200 cm^{-1} region show that ethylene bands at 3124, 3077, and 2988 cm^{-1} depleted as ethane bands near 2954 and 2894 cm^{-1} increased in intensity. The simultaneous formation of propionaldehyde and ethane indicates that the insertion of CO into adsorbed ethylene competes with ethylene hydrogenation.

Figure 8 shows the reaction of C_2H_4 and H_2 with the preadsorbed CO on the oxidized Rh/SiO$_2$ catalyst at 301 K. The infrared spectrum of adsorbed CO prior to exposure to C_2H_4 and H_2 is identical to that shown in Fig. 4. Admission of C_2H_4/H_2 to the preadsorbed CO resulted in the formation of the propionaldehyde band at 1732 cm^{-1} and a band at 1632 cm^{-1} and a dramatic variation of CO bands in the 2105–1860 cm^{-1} region. No bands that can be attributed to an adsorbed acyl species or complex were observed. The 1631 cm^{-1} band may be assigned to the carboxylate species of which carbon attaches on two oxygen atoms (*42*). The role of this species in the propionaldehyde formation remains unclear.

The change in IR spectra of adsorbed CO upon admission of C_2H_4/H_2 and during the

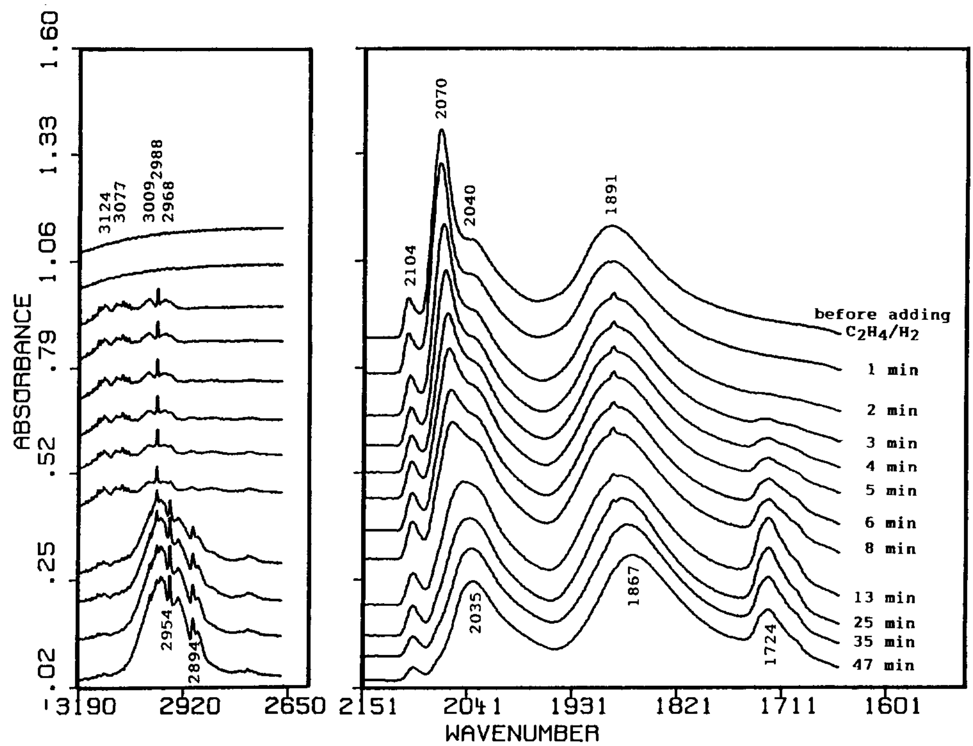

FIG. 7. Reaction of C_2H_4/H_2 with adsorbed CO on the reduced Rh/SiO_2 catalyst at 301 K.

reaction can be clearly discerned by the difference spectra as shown in Fig. 9. The difference spectrum 9a shows a very complex pattern, which is the mirror image of spectrum 5e. The unknown species exhibiting the complex spectrum disappeared upon admission of C_2H_4 and H_2. The species appears to be unstable under reaction conditions; its relation to propionaldehyde formation remains unclear. A clear relationship between the variation of adsorbed CO and the formation of propionaldehyde can be observed after 3 min of the reaction. The decrease in the band intensity at 2106 cm^{-1} appears to correlate to the increase in the propionaldehyde band intensity at 1732 cm^{-1}, suggesting that the linear CO adsorbed on the Rh^+ site is involved in CO insertion leading to the formation of propionaldehyde.

Figure 10 shows the changes of infrared spectra taken during the interaction of C_2H_4 and H_2 with preadsorbed CO on the sulfided Rh/SiO_2 catalyst at 301 K. The intensity of the linear CO at 2091 cm^{-1} decreased upon the addition of C_2H_4 and H_2. Neither detectable propionaldehyde nor ethane was observed during the entire period of the reaction study. The lack of activity of the sulfided catalyst for catalyzing propionaldehyde and hydrocarbon formation may be due to a strong inhibition of ethylene and hydrogen adsorption brought about by adsorbed sulfur at 301 K.

Steady-State Ethylene Hydroformylation

Figure 11 shows the infrared spectra for ethylene hydroformylation on the reduced Rh/SiO_2 catalyst. The rates of product formation corresponding to the infrared spectra are presented in Table 1. Ethane was the major product; methane and propionaldehyde were minor products at 373 K and 1 atm. Under the same reaction condition, the

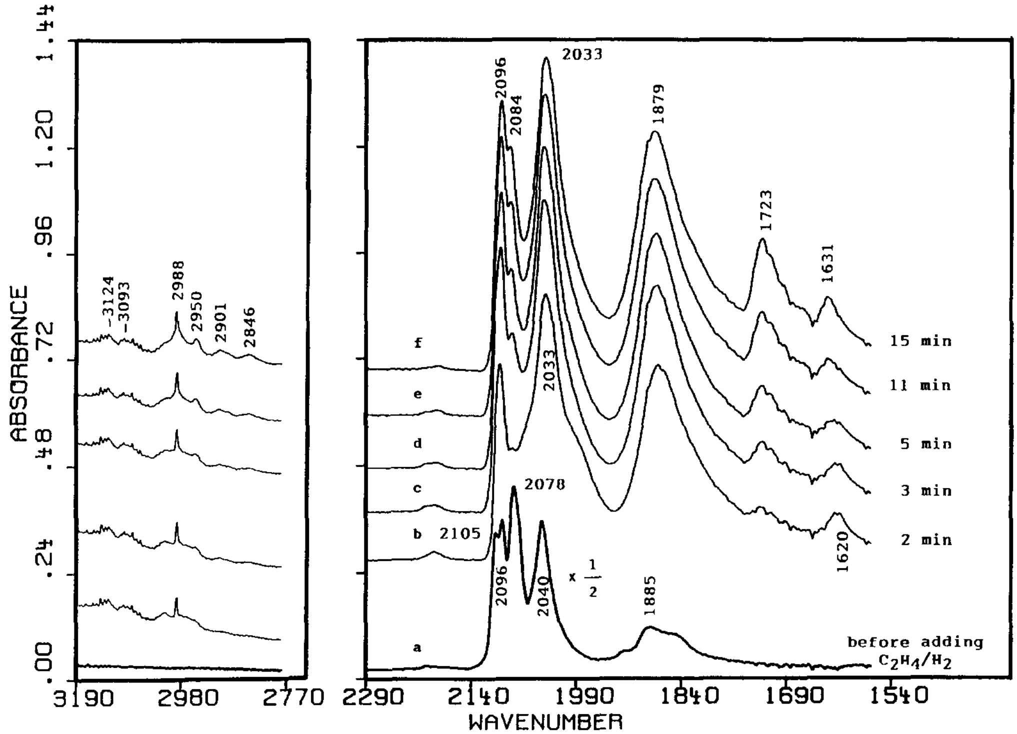

FIG. 8. Reaction of C_2H_4/H_2 with adsorbed CO on the oxidized Rh/SiO_2 catalyst at 301 K.

infrared spectrum shows the prominent linear CO band at 2042 cm^{-1} and the bridge CO band at 1871 cm^{-1}. Increasing temperature from 373 to 513 K at 1 atm resulted in a significant increase in the rate of formation of ethane and propionaldehyde and a slight increase in the selectivity toward propionaldehyde. Increasing the reaction temperature also reduced the intensity and wavenumber of the linear CO and bridged CO bands, but increased the intensity of hydrocarbon bands. A wavenumber decrease for the linear CO and bridge CO has been attributed to a decrease in the dipole–dipole coupling between adsorbed CO (*37*) as a result of the dilution of adsorbed CO by adsorbed propionaldehyde and hydrocarbons.

Subsequent increases in pressure from 1 to 10 atm at 573 K further increased the rates of formation for methane, ethane, and propionaldehyde by factors of about 4.6, 8, and 17.5, respectively. The use of high pressures significantly enhanced the selectivity to propionaldehyde. The increases in pressure also caused a slight increase in the intensity of the linear CO band, the formation of the propionaldehyde band at 1730 cm^{-1}, and the development of intense ethane bands at 2946 and 2890 cm^{-1}. No infrared evidence of CO adsorbed on Rh^+ ions was observed during the entire course of reaction studies on the reduced Rh/SiO_2.

Figure 12 shows the infrared spectra as a function of time for ethylene hydroformylation on the oxidized Rh/SiO_2 catalyst at 373 K and 1 atm. Low reaction temperature and pressure were used to prevent the oxidized Rh surface from complete reduction. The rate of product formation corresponding to the IR spectra is listed in Table 1. Ethane, propionaldehyde, and methane were the major products. The infrared spectrum corresponding to the rate data showed the propionaldehyde band at 1733 cm^{-1}, the bridge

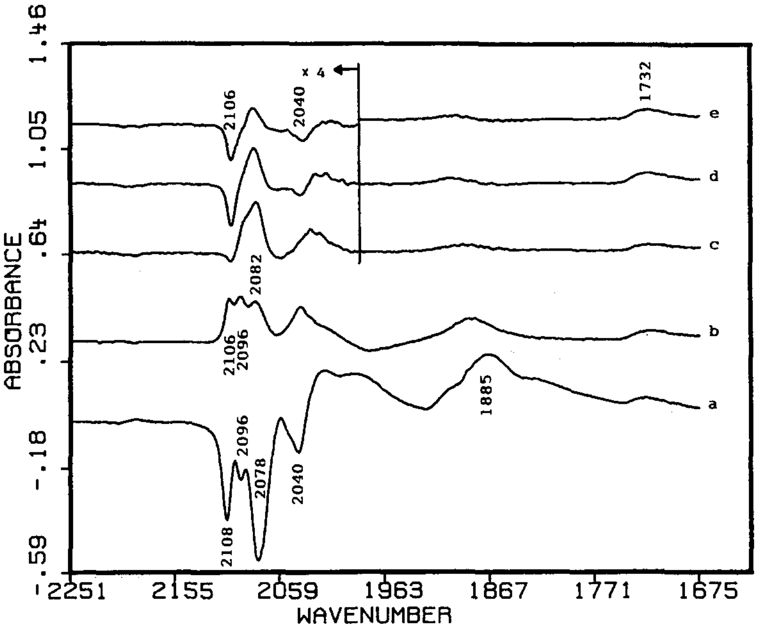

FIG. 9. Sequential difference spectrum of the reaction of C_2H_4/H_2 with adsorbed CO obtained from subtraction of spectra in Fig. 8; spectrum 9a = 8b − 8a, spectrum 9b = 8c − 8b, spectrum 9c = 8d − 8c, etc.

CO band at 1881–1886 cm^{-1}, a sharp peak at 2083 cm^{-1}, and a broad band at 2025–2033 cm^{-1}. The wavenumbers of the two latter bands fall in the range of rhodium gem dicarbonyl. The unusually high ratio of integrated intensities of these bands at 2033 and 2083 cm^{-1} and the downward shift of the 2033 cm^{-1} band as its intensity decreases suggest that the 2033 cm^{-1} band is due to overlapping of the asymmetric band of gem dicarbonyl with other CO bands. Adsorbed species that exhibit IR bands in the 2025–2033 cm^{-1} range include carbonyl hydride and linear CO (*45*). The band in the 2020–2048 cm^{-1} range has been assigned to a carbonyl hydride species in a number of studies on the adsorption of H_2CO, D_2CO, and coadsorption of CO and H_2 on the Rh catalyst (*43–45*). The downward shift of the 2033 cm^{-1} band to 2025 cm^{-1} as the intensity decreased suggests the presence of the linear CO adsorbed on the Rh crystallite. The low wavenumber of the linear CO band formed at 2025 cm^{-1} can be attributed to the decrease in dipole–dipole interaction between adsorbed CO (*32, 37, 38*) as a result of adsorbed CO dilution by adsorbed ethylene and propionaldehyde.

The presence of the bridged CO band at 1866 cm^{-1} as well as the formation of CO_2 (at 2360 and 2340 cm^{-1}) on the oxidized Rh/SiO_2 indicates that the oxidized Rh surface was partially reduced during the reaction. The 1560 cm^{-1} band and the 1410 cm^{-1} band (not shown in Fig. 12) may be assigned to the bidentate of which oxygen atoms attach on a surface metal atom (*42, 46, 47*). Studies on C_2 oxygenate synthesis over Rh/TiO_2 and Mn–Rh/SiO_2 have suggested that the bidentate species is the reaction intermediate for the formation of C_2 oxygenates (*46, 47*). In contrast, Fukushima *et al.*(*48*) have proposed that the bidentate species is formed from the spillover of an adsorbed acetyl species on the Rh metal to the oxide. The propionaldehyde band at 1733 cm^{-1} and the ethane bands at 2950–2890 cm^{-1} decreased slightly in intensity with reaction time while

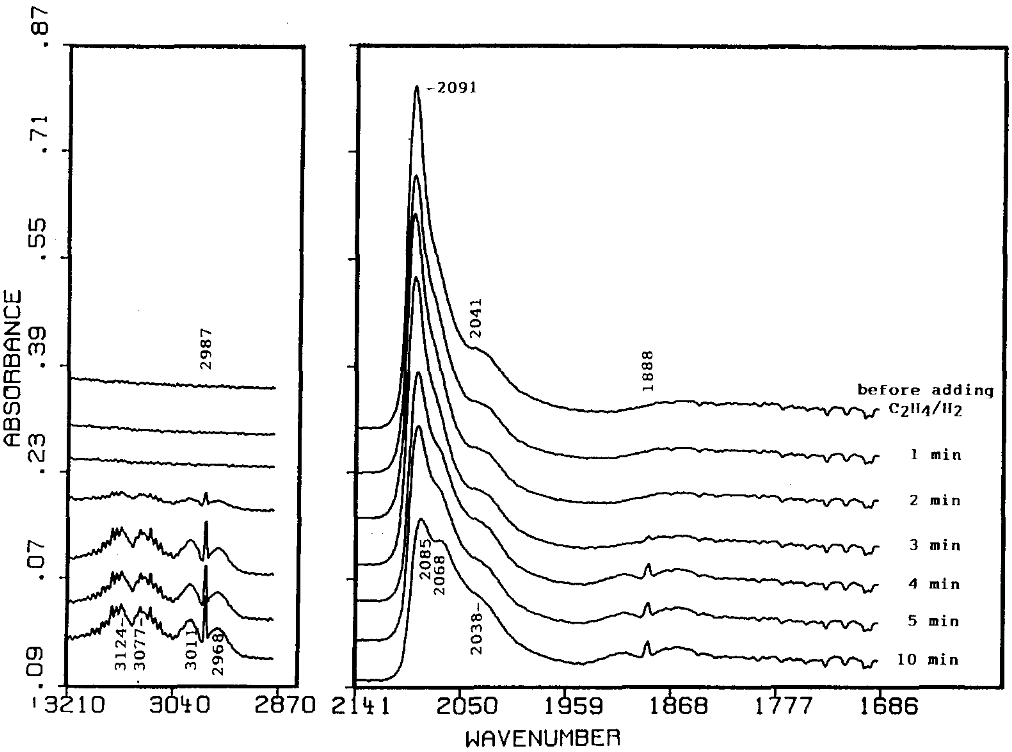

FIG. 10. Reaction of C_2H_4/H_2 with adsorbed CO on the sulfided Rh/SiO$_2$ catalyst at 301 K.

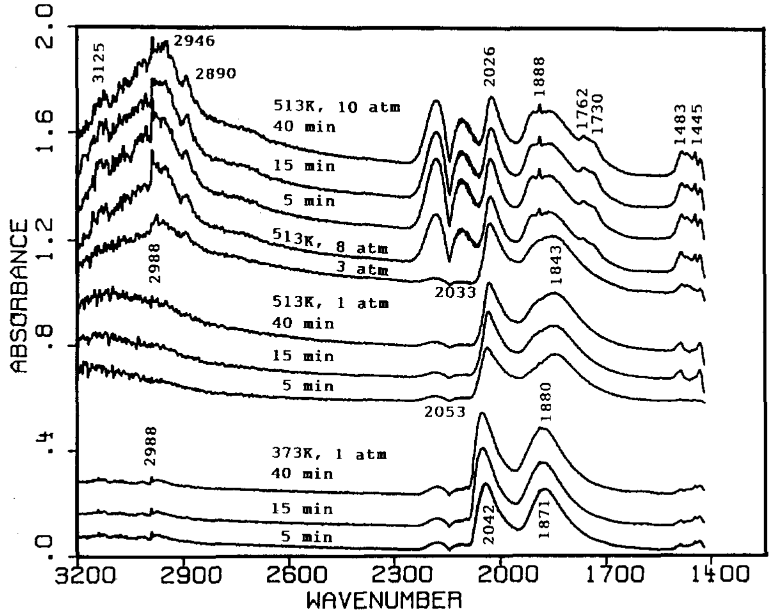

FIG. 11. Ethylene hydroformylation on the reduced Rh/SiO$_2$ catalyst.

TABLE 1

Rates of Product Formation for Ethylene Hydroformylation over Reduced, Oxidized, and Sulfided Rh/SiO$_2$ Catalysts

Catalyst/reaction condition	Rate of product formation (mol/Kg-h)					C_2H_5CHO/C_2H_6[a]
	CH_4	C_2H_6	C_{3+} HC	CH_3CHO	C_2H_5CHO	
			Reduced Rh/SiO$_2$			
373 K, 1 atm	0.025	0.14	—	—	0.016 (8.8)[b]	0.11
513 K, 1 atm	0.037	8.27	0.098	0.097	1.4 (14.1)	0.17
513 K, 10 atm	0.17	66.4	0.094	0.075	24.5 (26.8)	0.37
			Oxidized Rh/SiO$_2$			
373 K, 1 atm	0.012	0.075	—	—	0.025 (22.3)	0.33
			Sulfided Rh/SiO$_2$[c]			
373 K, 1 atm	0.013	0.001	—	—	—	0
513 K, 1 atm	0.023	2.5	—	—	0.43 (14.6)	0.17
513 K, 10 atm	0.094	48.9	0.092	—	27.0 (35.5)	0.55

[a] The ratio of the rate of product formation.

[b] The selectivity of propionaldehyde (mol%).

[c] The bulk ratio of S to Rh = 0.12.

the bidentate band at 1560 cm^{-1} remained constant during the reaction. The propionaldehyde band observed on the oxidized Rh/SiO$_2$ is significantly more intense than that on the reduced Rh/SiO$_2$ (shown in Fig. 11). The results are consistent with the consider-

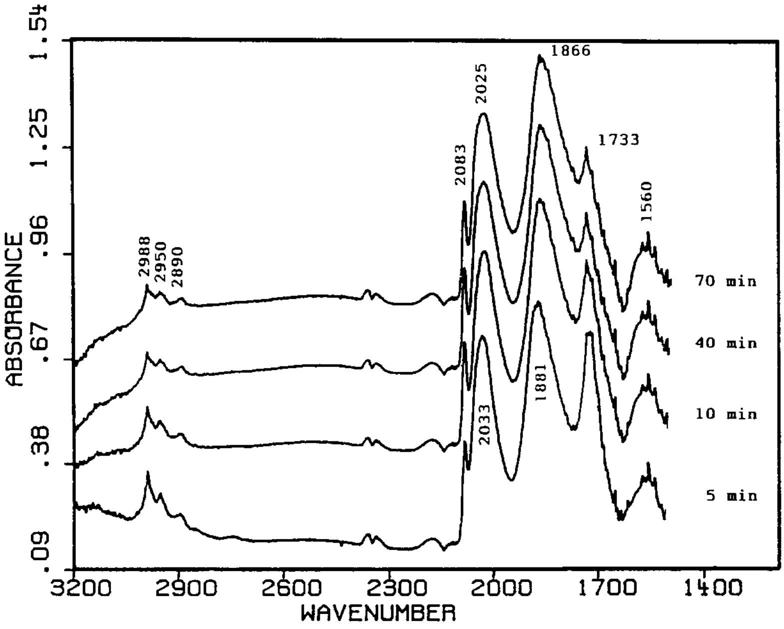

FIG. 12. Ethylene hydroformylation on the oxidized Rh/SiO$_2$ catalyst.

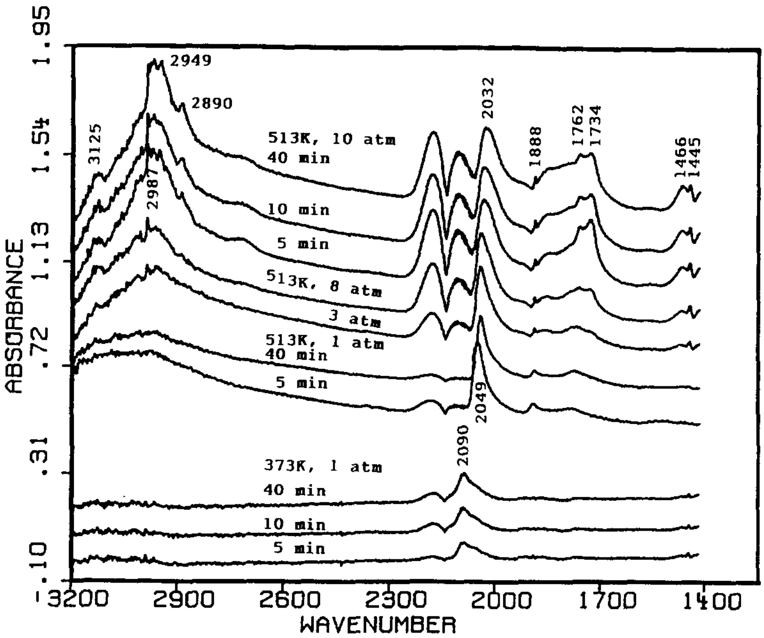

FIG. 13. Ethylene hydroformylation on the sulfided Rh/SiO$_2$ catalyst.

ably high propionaldehyde selectivity observed on the oxidized Rh/SiO$_2$ compared to the reduced Rh/SiO$_2$.

Figure 13 shows the infrared spectra of ethylene hydroformylation on the sulfided Rh/SiO$_2$. The rate of product formation is listed in Table 1. At 373 K and 1 atm, the linear CO at 2090 cm^{-1} was the only adsorbed CO on the catalyst; methane and ethane were the observed products. Increasing the reaction temperature from 373 to 513 K at 1 atm resulted in propionaldehyde formation and a rate increase for hydrocarbon formation. The temperature increase also caused an increase in the linear CO band intensity and an emergence of weak propionaldehyde and hydrocarbon bands. Subsequent increases in reaction pressure from 1 to 10 atm at 513 K slightly increased the intensities of the linear CO and further enhanced the intensity of the propionaldehyde and hydrocarbon bands; the increasing pressure also increased the formation rates of methane, ethane, and propionaldehyde by a factor of 4, 19.5, and 62.8, respectively. High pressure greatly enhanced the rate and selectivity for the formation of propionaldehyde.

DISCUSSION

Characterization of the Rh Surface by Infrared Spectroscopy of CO Adsorption

The types of CO adsorbed on the Rh catalysts are very sensitive to the structure and chemical environment of the Rh surface. It has been well established that the reduced Rh crystallite surface chemisorbs CO as linear and bridge CO species; the oxidized Rh surface contains isolated Rh$^+$sites that adsorb CO as gem dicarbonyl (*28–35*). The sulfided Rh surface also possesses isolated Rh sites, which have been suggested to carry positive charges; these sites chemisorb CO as linear CO or gem dicarbonyl (*39*).

Three types of adsorbed CO species including linear CO, bridge CO, and gem dicarbonyl were clearly observed from the spectra of CO adsorbed on the reduced Rh/SiO_2 catalyst, as shown in Fig. 3. The results indicate that the surface of the reduced Rh/SiO_2 contains both reduced Rh crystallite and isolated Rh^+ sites. XPS studies revealed that the surface of reduced Rh/SiO_2 prior to CO adsorption contains primarily the reduced Rh^0 atoms. The observation of gem dicarbonyl suggests that CO adsorption led to the formation of isolated Rh^+ sites on the reduced Rh/SiO_2. The formation of $Rh^+(CO)_2$ from adsorption of CO on Rh^0 sites has been found to involve isolated OH groups. The process can be reversed by hydrogen treatment (*35, 49, 50*).

XPS studies (shown in Fig. 2) have shown that oxidation of the reduced Rh/SiO_2 at 513 K produced the oxidized Rh/SiO_2, the surface of which contains primarily Rh^+ ions. CO adsorption on the oxidized Rh/SiO_2 produced linear CO and gem dicarbonyl adsorbed on the isolated Rh^+ ions. Increasing CO pressures led to the formation of bridge CO adsorbed on Rh crystallites as well as the formation of an unknown CO species. The formation of bridge CO indicates that part of the oxidized Rh surface was reduced during CO adsorption.

CO Insertion

The metal carbonyl hydrides play a central role in the catalytic chemistry of CO insertion (*51*). Metal carbonyl hydride such as $HCo(CO)_4$ can protonate methanol resulting in the formation of methyl cobalt intermediates and the subsequent migratory CO insertion leading to the formation of ethanol. The labile nature of the *M*–H bond in the metal carbonyl hydride also permits olefin insertion leading to the formation of an alkyl metal intermediate; the following migration of the alkyl group to the carbon of the CO ligand (also known as the migratory CO insertion) resulted in the formation of an acyl intermediates (*1, 2*),

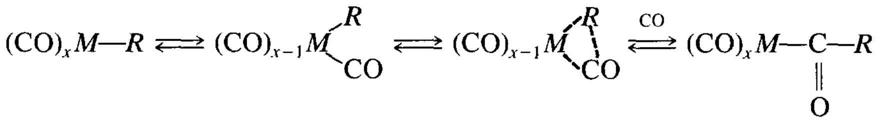

$$(CO)_xM{-}R \rightleftharpoons (CO)_{x-1}M(R)(CO) \rightleftharpoons (CO)_{x-1}M(R \cdots CO) \overset{CO}{\rightleftharpoons} (CO)_xM{-}C({=}O){-}R$$

(*R* is an alkyl group and *M* is a metal). In the process of the migratory CO insertion, the metal center of the carbonyl species maintains its oxidation state of +1 (*1, 51*). The reaction has been observed for all group VIII metal carbonyls and complexes (*1*).

The apparent analogy between the well-defined organometallic reaction steps and the elementary step on the heterogeneous catalyst surface has been used as a basis for the development of CO insertion mechanism on the surface of supported Rh catalysts (*9, 19, 52*). The suggested pathway for the CO insertion in ethylene hydroformylation over supported Rh catalysts is presented in Fig. 14 (*19, 53*). The formation of propionaldehyde involves three major steps: hydrogenation of adsorbed C_2H_4 to form adsorbed ethyl species, insertion of adsorbed CO into $*C_2H_5$ to form adsorbed acyl species, and then hydrogenation to produce propionaldehyde. The occurrence of migratory CO insertion on the metal center with an oxidation state of +1 in organometallic chemistry suggests that CO insertion may also take place on the Rh^+ site on the supported Rh catalyst (*54*). The mechanism involving CO insertion on the Rh^+ sites has been proposed on the basis of the following observations: (i) preoxidation of Rh foil increased the initial rates and selectivity for the formation of oxygenates from CO hydrogenation and ethylene addition (*16*), and (ii) the catalysts containing Rh^+ ions exhibited higher rates for C_2 oxygenate synthesis and ethylene hydroformylation than those con-

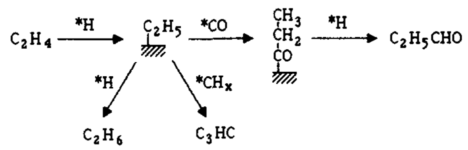

FIG. 14. The reaction pathway for ethylene hydroformylation on supported Rh catalysts. (*H) Adsorbed hydrogen; (*CO) adsorbed carbon monoxide; (*CH_x) adsorbed CH_x species; (HC) hydrocarbon.

taining Rh^0 (*16, 17, 19, 23, 54*). On the contrary, lack of correlation of the activity for C_{2+} oxygenate synthesis and ethylene hydroformylaton to the Rh^+ concentration has been reported in a number of studies (*25–27*). It should be noted that the sites for C_2 oxygenate synthesis include CO dissociation, hydrogenation, and CO insertion sites, while ethylene hydroformylation occurs on hydrogenation and CO insertion sites. The catalysts that are active for ethylene hydroformylation generally show high selectivity for C_2 oxygenate synthesis (*15, 16, 19, 26, 53, 56, 57*).

The correlation between the formation of propionaldehyde and consumption of specific forms of adsorbed CO should permit unequivocal identification of the forms of CO involved in the CO insertion leading to the formation of propionaldehyde. The direct correlation between the propionaldehyde production and the linear CO consumption observed in Figs. 7 and 9 indicated that linear CO adosrbed on the Rh^0 site participates in CO insertion on the reduced Rh/SiO$_2$; linear CO adsorbed on the Rh^+ site takes part in CO insertion on the oxidized Rh/SiO$_2$. Other adsorbed CO species including gem dicarbonyl and bridge CO serve as spectator species that are not involved in the reaction. Comparison of the rate of growth of propionaldehyde bands in Figs. 7 and 8 shows that the oxidized Rh/SiO$_2$ is more active for catalyzing the formation of propionaldehyde than the reduced Rh/SiO$_2$ suggesting that Rh^+ sites are more active for CO insertion than Rh^0 sites.

The dominant CO species observed during ethylene hydroformylation on the reduced Rh/SiO$_2$ are the linear CO and bridge CO adsorbed on the Rh^0 crystallite sites. The high rate of ethane formation and the low rate of propionaldehyde formation on the reduced Rh/SiO$_2$ as compared to the oxidized and sulfided Rh/SiO$_2$ catalyst can be attributed to the high hydrogenation activity of Rh crystallite surface. The variation of reaction temperatures and pressures from 373 K and 1 atm of 513 K and 10 atm has little influence on the adsorbed CO. Comparison of the wavenumbers of linear CO in Figs. 7 and 11 shows that the linear CO under hydroformylation conditions exhibits lower wavenumbers than those observed under CO adsorption. This is primarily due to the dilution of adsorbed CO by adsorbed reactants and products. The dilution effect can be further confirmed by the observation that the decreasing wavenumber and intensity of the linear CO band is accompanied by the growing hydrocarbon and propionaldehyde bands shown in Fig. 11.

The gem dicarbonyl on the Rh^+ sites as well the linear CO and bridge CO on the Rh^0 sites are the major adsorbed CO species during ethylene hydroformylation on the oxidized Rh/SiO$_2$. The results indicate that both Rh^+ and Rh^0 sites are present on the oxidized Rh/SiO$_2$ during the reaction. Due to the lack of information on the number of active sites on the reduced Rh and oxidized Rh catalysts, direct comparison of the activity of these two catalysts is not possible. In spite of the surface of the oxidized Rh/SiO$_2$ containing a considerable amount of Rh^0 sites, the oxidized Rh/SiO$_2$ catalyst exhibited higher selectivity to propionaldehyde than the reduced Rh/SiO$_2$ in steady-state ethylene hydroformylation. The high activity and selectivity of the oxidized Rh/SiO$_2$ appear to be due to the presence of Rh^+ sites on the catalyst. Our results are in good agreement with previous reports for the catalysts containing Rh^+ sites that exhibited high selectivity for C_2 oxygenate synthesis and ethylene hydroformulation (*15, 17, 19, 23, 54*).

The different conclusions drawn from

various studies on the active site for CO insertion can be reconciled by results of the present study. Results of this study have shown that both single Rh^0 atoms and single Rh^+ ions are active for CO insertion. The observation of Rh^0-catalyzing CO insertion is in good agreement with previously observed high C_2 oxygenate synthesis and hydroformylation activities for $LaRhO_3$ and Rh/V_2O_3, which contain only Rh^0 sites (*25–27*). It is likely that the Rh^0 on the surface of these catalysts is also in a single atom state.

The important role of the single Rh atom site in CO insertion can be demonstrated by the high selectivity and activity of the sulfided Rh/SiO_2 for ethylene hydroformylation. The bridge CO sites can be blocked by adsorbed sulfur (*55*) resulting in the formation of isolated Rh sites, which give rise only to linear CO as shown in Fig. 6. Comparison of the rate data and IR data for the reduced and sulfided Rh/SiO_2 catalysts shows that the rate, selectivity, and infrared intensity for propionaldehyde are greater on the sulfided Rh than on the reduced Rh at 513 K and 10 atm. Adsorbed sulfur also shifts the wavenumber of linear CO to higher wavenumber indicating that adsorbed sulfur makes the neighboring Rh atom more electropositive. In spite of its high activity and selectivity for ethylene hydroformylation, the sulfided Rh/SiO_2 exhibited little reactivity for the reaction of C_2H_4 and H_2 with adsorbed CO at 301 K as a result of the inhibition of C_2H_4/H_2 adsorption brought about by adsorbed sulfur.

Additives including Ag (*53*), Zn (*58*), Ti, and Fe (*59*) have been found to block bridge CO sites. The blockage of bridge CO sites by these additives increases the ratio of the linear CO to bridge CO sites resulting in enhancement of CO insertion selectivity. Ponec and co-workers (*27*) have suggested that the blocking of the Rh surface by supports such as V_2O_3 could result in the suppression of hydrocarbon formation and the enhancement of the selectivity for C_2 oxygenate synthesis. In addition to the site blockage of additives, other possible effects of additives on C_2 oxygenate synthesis include: stabilization of Rh^{n+} sites, activation of CO by oxophilic additives (Mn and Zr), and stabilization of the oxygenated intermediates (*60, 61*).

Although the reduced, oxidized, and sulfided Rh/SiO_2 catalysts exhibit CO insertion activity, the selectivity of these catalysts for the CO insertion reaction remains significantly lower than that of Rh carbonyls and complexes that have long been used for commercial hydroformylation and carbonylation (*1–5*). An understanding of the role of CO insertion sites in hydrogenation, the side reaction of hydroformylation, is essential for the improvement of selectivity of heterogeneously supported metal catalysts for the CO insertion-related reactions.

CONCLUSIONS

The linear CO species adsorbed on both single Rh^0 atom and Rh^+ ion sites have been found to participate in CO insertion leading to the formation of propionaldehyde from C_2H_4 and H_2. The linear CO on the Rh^+ site of the oxidized Rh/SiO_2 appears to be more active for CO insertion than that on the reduced Rh^0 site of the reduced Rh/SiO_2. These results show that both single Rh^0 atom and Rh^+ ion sites serve as active sites for CO insertion. The CO species observed under ethylene hydroformylation conditions are the linear CO and bridge CO on the Rh^0 crystallite surface of the reduced Rh/SiO_2, gem dicarbonyl on the Rh^+ sites, as well as the linear CO and bridge CO on the Rh^0 crystallite surface of the oxidized Rh/SiO_2, and the linear CO on the sulfided Rh/SiO_2. In addition, a species that can be assigned to carbonyl hydride is present on the surface of the oxidized Rh/SiO_2 under hydroformylation conditions. However, the state of Rh atom that associates with the species remains unclear.

The oxidized Rh/SiO_2 exhibits higher rates and selectivities for the formation of propionaldehyde than the reduced Rh/SiO_2 at 313 K and 1 atm; under high pressure and temperature (513 K and 10 atm) the sulfided Rh/SiO$_2$ exhibits higher rates and selectivities for the formation of propionaldehyde than the reduced Rh/SiO$_2$. The difference in activity and selectivity of these catalysts for ethylene hydroformylation can be attributed to the different surface states of Rh on these catalysts. Both the electronic state and the geometric structure (size of ensembles) of surface Rh atoms play important roles in determining CO insertion activity and selectivity.

ACKNOWLEDGMENTS

We gratefully acknowledge the partial support of this research by the U.S. Department of Energy (DG-FG-87PC79923) and the Research Challenge Program of the Ohio Board of Regents. We thank Dr. J. Baltrus at PETC for performing XPS studies.

REFERENCES

1. Calderazzo, F., *Angew. Chem. Int. Ed. Engl.* **16,** 299 (1977).
2. Cross, R. J., *in* "Catalysis" (G. C. Bond and G. Webb, Eds.), Vol. 5, p. 366. The Royal Society of Chemistry, London, 1982.
3. Parshall, G. W., "Homogeneous Catalysis—The Applications and Chemistry of Catalysis by Soluble Transition Metal Complexes," p. 85. Wiley, New York, 1981.
4. Masters, C., "Homogeneous Transition-Metal Catalysis—A Gentle Art," p. 102. Chapman & Hall, New York, 1891.
5. Pino, P., Piacenti, F., and Bianchi, M., *in* "Organic Synthesis via Metal Carbonyls" (I. Wender and P. Pino, Eds.), Vol. 2, p. 43. Wiley, New York, 1977.
6. Noack, K., and Calderazzo, F., *J. Organometal. Chem.* **10,** 101 (1967).
7. Butts, S. B., Strauss, S. H., Holt, E. M., Stimson, R. E., Alcok, N. W., and Shriver, D. E., *J. Am. Chem. Soc.* **102,** 5093 (1980).
8. Pichler, H., Schulz, H., and Elstner, M., *Brennst Chem.* **48,** 78 (1967).
9. Henrici-Olive, G., and Olive, S., "The Chemistry of the Catalyzed Hydrogenation of Carbon Monoxide." Springer-Verlag, New York, 1984.
10. Biloen, P., and Sachtler, W. M. H., *in* "Advances in Catalysis" (D. D. Eley, H. Pines, and P. B. Weisz, Eds.), Vol. 30, p. 165. Academic Press, New York, 1981.
11. Bell, A. T., *Catal. Rev. Sci. Eng.* **23,** 203 (1981).
12. Ponec, V., *in* "Catalysis" (G. C. Bond and G. Webb, Eds.), Vol. 5, p. 48. The Royal Society of Chemistry, London, 1982.
13. Anderson, R. B., "Fischer Tropsch and Related Syntheses." Academic Press, New York, 1983.
14. Cotton, F. A., and Wilkinson, G., "Advanced Inorganic Chemistry," p. 1233. Wiley, 1988.
15. Chuang, S. C., Tian, Y. H., Goodwin, J. G., Jr., and Wender, I., *J. Catal.* **96,** 396 (1985).
16. Watson, P. R., and Somorjai, G. A., *J. Catal.* **72,** 347 (1981).
17. Watson, P. R., and Somorjai, G. A., *J. Catal.* **74,** 282 (1982).
18. Ichikawa, M., *Chemtech,* 674 (1982).
19. Sachtler, W. M. H., and Ichikawa, M., *J. Phys. Chem.* **90,** 4752 (1986).
20. Van der Berg, F. G. A., Ph.D. thesis, University of Leiden, The Netherlands, 1984.
21. Underwood, R. P., and Bell, A. T., *J. Catal.* **111,** 325 (1988).
22. Castner, D. G., Blackadar, R. L., and Somorjai, G. A., *J. Catal.* **66,** 257 (1980).
23. Kawai, M., Uda, M., and Ichikawa, M., *J. Phys. Chem.* **89,** 1654 (1985).
24. Wilson, T. P., Kasai, P. H., and Ellgen, P. C., *J. Catal.* **69,** 193 (1981).
25. Katzer, J. R., Sleight, A. W., Gajarsdo, P., Michel, J. B., Gleason, E. F., and McMillian, S., *Faraday Discuss. Chem. Soc.* **72,** 121 (1981).
26. Gysling, H. J., Monnier, J. R., and Apai, G., *J. Catal.* **103,** 407 (1987).
27. van der Lee, G., Schuller, B., Post, T., Favre, T. L. F., and Ponec, V., *J. Catal.* **98,** 522 (1986).
28. Yang, A. C., and Garland, C. W., *J. Phys. Chem.* **61,** 1504 (1957).
29. Yates, J. T., Jr., Duncan, T. M., Worley, S. D., and Vaughn, R. W., *J. Chem. Phys.* **70,** 1219 (1979).
30. Cavanagh, R. R., and Yates, J. T., Jr., *J. Chem. Phys.* **74,** 4150 (1981).
31. Solymosi, F., Tombacz, I., and Kocsis, M., *J. Catal.* **75,** 78 (1982).
32. Rice, C. A., Worley, S. D., Curtis, C. W., Guin, J. A., and Tarrer, A. R., *J. Chem. Phys.* **74,** 6487 (1981).
33. Worley, S. D., Rice, C. A., Matson, G. A., Curtis, C. W., Guin, J. A., and Tarrer, A. R., *J. Chem. Phys.* **76,** 20 (1982).
34. Worley, S. D., Rice, C. A., Mattson, G. A., Curtis, C. W., Guin, J. A., and Tarrer, A. R., *J. Phys. Chem.* **86,** 2714 (1982).
35. Solymosi, F., and Pasztor, M., *J. Phys. Chem.* **89,** 4789 (1985).
36. van't Blik, H. F. J., van Zon, J. B. A. D., Huizinga, T., Vis, J. C., Koningsberger, D. C., and Prins, R., *J. Phys. Chem.* **87,** 2264 (1983).
37. Stoop, F., Toolenaar, F. J. C. M., and Ponec, V., *J. Catal.* **70,** 50 (1982).
38. Angevaare, P. A. J. M., Henderickx, H. A. C. M., and Ponec, V., *J. Catal.* **110,** 18 (1988).
39. Konishi, Y., Ichikawa, M., and Sachtler, W. M. H., *J. Phys. Chem.* **91,** 6286 (1987).
40. Li, Y. E., and Gonzalez, R. D., *J. Phys. Chem.* **92,** 1589 (1988).

41. Rode, E. J., Davis, M. E., and Hanson, B. E., *J. Catal.* **96,** 574 (1985).
42. Hair, M. L., "Infrared Spectroscopy in Surface Chemistry." Dekker, New York, 1967.
43. Yates, J. T., Jr., Worley, S. D., Duncan, T. M., and Vaughan, R. W., *J. Phys. Chem.* **70,** 1225 (1979).
44. Worley, S. D., Mattson, G. A., and Caudill, R., *J. Phys. Chem.* **87,** 1671 (1983).
45. Solymosi, F., and Pasztor, M., *J. Phys. Chem.* **90,** 5312 (1986).
46. Orita, H., Naito, S., and Tamaru, K., *J. Catal.* **90,** 183 (1984).
47. Orita, H., Naito, S., and Tamaru, K., *J. Phys. Chem.* **89,** 3066 (1985).
48. Fukushima, T., Arakawa, H., and Ichikawa, M., *J. Chem. Soc. Chem. Commun.*, 729 (1985).
49. Basu, P., Panayotov, D., and Yates, J. T., Jr., *J. Phys. Chem.* **91,** 3113 (1987).
50. Basu, P., Panayotov, D., and Yates, J. T., Jr., *J. Am. Chem. Soc.* **110,** 2074 (1988).
51. Sheldon, R. A., "Chemicals from Synthesis Gas." Riedel, Boston, 1983.
52. Chuang, S. S. C., and Pien, S. I., *J. Mol. Catal.* **55,** 12 (1989).
53. Chuang, S. S. C., Pien, S. I., and Narayanan, R., *Appl. Catal.* **57,** 241 (1990).
54. van den Berg, F. G. A., Glezer, J. H. E., and Sachtler, W. M. H., *J. Catal.* **93,** 340 (1985).
55. Chuang, S. S. C., Pien, S. I., and Sze, C., *J. Catal.* **126,** 187 (1990).
56. Lou, H. Y., Bastein, A. G. T. M., Mulder, A. A. J. P., and Ponec, V., *Appl. Catal.* **38,** 241 (1988).
57. Chuang, S. S. C., and Pien, S. I., *J. Catal.* **128,** 569 (1991).
58. Ichikawa, M., Lang, A. J., Shriver, D. F., and Sachtler, W. M. H., *J. Am. Chem. Soc.* **107,** 7216 (1985).
59. Arakawa, H., Hanaoka, T., Takeuchi, K., Matsuzaki, T., and Sugi, Y., *in* "Proceedings, 9th International Congress on Catalysis, Calgary, 1988" (M. J. Phillips and M. Ternan, Eds.), Vol. 2, p. 602. Chem. Institute of Canada, Ottawa, 1988.
60. Lavalley, J. C., Saussey, J., Lamotte, J., Breault, R., Hindermann, J. P., and Kiennemann, A., *J. Phys. Chem.* **94,** 5941 (1990).
61. Sachtler, W. M. H., *in* "Proceedings, 8th International Congress on Catalysis, Berlin, 1984" (G. Ertl, Ed.), Vol. 1, p. 151. Dechema, Frankfurt-am-Main, 1984.